

This is an Open Access document downloaded from ORCA, Cardiff University's institutional repository: <https://orca.cardiff.ac.uk/id/eprint/122575/>

This is the author's version of a work that was submitted to / accepted for publication.

Citation for final published version:

Hellier, Pip, Wells, Peter P and Bowker, Michael 2019. Methanol oxidation over shell-core MO_x/Fe₂O₃ (M = Mo, V, Nb) catalysts. Chinese Journal of Catalysis 40 (11) , pp. 1686-1692. 10.1016/S1872-2067(19)63350-4

Publishers page: [https://doi.org/10.1016/S1872-2067\(19\)63350-4](https://doi.org/10.1016/S1872-2067(19)63350-4)

Please note:

Changes made as a result of publishing processes such as copy-editing, formatting and page numbers may not be reflected in this version. For the definitive version of this publication, please refer to the published source. You are advised to consult the publisher's version if you wish to cite this paper.

This version is being made available in accordance with publisher policies. See <http://orca.cf.ac.uk/policies.html> for usage policies. Copyright and moral rights for publications made available in ORCA are retained by the copyright holders.



Methanol oxidation over shell-core $\text{MO}_x/\text{Fe}_2\text{O}_3$ ($\text{M} = \text{Mo}, \text{V}, \text{Nb}$) catalysts

Pip Hellier ^{a,b}, Peter P. Wells ^{c,d}, Michael Bowker ^{a,b,*}

^a UK Catalysis Hub, Research Complex at Harwell, Rutherford Appleton Laboratory, Harwell,

UK ^b School of Chemistry, Cardiff University, Cardiff, UK

^c School of Chemistry, University of Southampton, Southampton, UK

^d Diamond Light Source Ltd, Harwell Science and Innovation Campus, Didcot, UK

ARTICLE INFO

Keywords:

Methanol
Oxidation
Formaldehyde
Iron molybdate
Shell-core catalyst

ABSTRACT

We present a comparison of Mo, V and Nb oxides as shell materials atop haematite cores used for selective methanol oxidation. While Mo and V both yield high selectivity to formaldehyde, Nb does not. Very different reactivity patterns are seen for Nb, which mainly shows dehydrogenation (to CO) and dehydration (to DME), indicating the lack of a complete shell, while Raman spectroscopy shows that the Mo and V formation process is not followed by NbO_x . We suggest this is due to the large differences in mobility within the solid materials during formation, NbO_x requiring significantly higher (and deleterious) calcination temperatures to allow sufficient mobility for shell completion.

1. Introduction

Methanol is an important intermediate chemical and fuel, and it may have a significant role in CCU (carbon capture and utilisation) [1]. Thus, renewable electricity from wind and photovoltaic can be used to produce hydrogen, but due to its low energy density we may want to densify it in the form of a liquid fuel such as methanol. A demonstrator plant for such a process is in place in Germany through a European collaboration [2]. Since formaldehyde is a derivative of methanol, we can then envisage a route to 'green' formaldehyde.

In this paper we describe the behaviour of mixed oxide catalysts for this process in which one cation is Fe^{3+} , and the other is M, where M is either Mo, V, or Nb. Mo is the cation of choice

and industrial catalysts are composed of ferric molybdate, $(\text{Fe}_2(\text{MoO}_4)_3)$ [3–5]. This material has very high selectivity at high conversion and hence its industrial significance [6]. Here we compare its behaviour with those of two high oxidation state cations nearby in the periodic table. We also utilise our model shell-core catalysts in which we put a shell of M on top of a haematite core (which forms the oxide shell during calcination) and we have shown that, at least in the case of Mo and V, it remains at the surface [7,8]. The aim of the work is to determine why Mo is the cation of choice for such catalysts by finding out how related cations compare in reactivity. Here we show that although V is good, it is not as effective as Mo in terms of selectivity and yield of formaldehyde, and that Nb differs considerably in reactivity from these two.

* Corresponding author. E-mail: bowkerm@cardiff.ac.uk

The authors thank HarwellXPS, the EPSRC National Facility for X-Ray Photoelectron Spectroscopy, for their assistance in performing XPS measurements, and EPSRC for support via the UK Catalysis Hub (EP/K014854/1, EP/K014714/1), and EPSRC and Diamond Light Source for funding the studentship to PH.

2. Experimental

2.1. Catalyst synthesis

1 ML $\text{MO}_x/\text{Fe}_2\text{O}_3$ catalysts (where $M = \text{Mo}, \text{Nb}$) were prepared by incipient wetness impregnation, in which the relevant amount of ammonium heptamolybdate, $(\text{NH}_4)_6\text{Mo}_7\text{O}_{24}$, or ammonium niobate oxalate hydrate, $\text{C}_{10}\text{H}_5\text{NbO}_{20} \cdot x\text{H}_2\text{O}$ (both Sigma-Aldrich, >99%), to achieve 1 ML coverage was dissolved in water and added dropwise to Fe_2O_3 (Sigma-Aldrich, nano-powder, 99%). MoO_3 and Nb_2O_5 references were obtained commercially. 1 ML $\text{VO}_x/\text{Fe}_2\text{O}_3$ catalysts were prepared by an analogous incipient wetness impregnation method, but with ethanolamine as the solvent and ammonium meta-vanadate, NH_4VO_3 , as the precursor. V_2O_5 was obtained commercially as a reference material. All reference compounds were calcined at 500 °C for 24 h in air before being used as references. The weight loadings of the second cations on the sample were Mo 2.56%, Nb 2.76% and V 1.62%.

2.2. Catalytic testing

TPD and selectivity/conversion analysis data were obtained from a Hiden CATLAB microreactor with online mass spectrometric analysis, consisting of a furnace around the sample through which gas passes. For TPD, methanol was injected in microlitre quantities (5) at room temperature, followed by heating to 500 °C under a He flow; for pulsed flow reactions (to determine selectivity and conversion), microlitre aliquots of methanol were injected every 2 min into a 30 mL min^{-1} flow of 10% O_2/He during a 10 °C min^{-1} ramp to 500 °C. Products of these processes were monitored by the online Hiden QGA quadrupole mass spectrometer during the temperature ramps. Figures using mass spectra data display processed data, i.e. post removal of spectral overlaps. The reproducibility of data was $\pm 5\%$ on conversion and on selectivity at any one temperature. The products shown in the figures are the only ones seen and the mass balance was 100 ($\pm 2\%$).

2.3. Characterisation

Vibrational spectroscopy was primarily used to identify component speciation at different calcination stages and after full calcination at 500 °C. Raman measurements were undertaken using a Renishaw Raman microscope with an 830 nm laser under ambient conditions, with typical measurements ranging between 300 and 1200 cm^{-1} with 1% laser power and 5 accumulations of 20 s each. XPS spectra were obtained using an ESCALAB 220 spectrometer equipped with Al $K\alpha$ and Mg $K\alpha$ sources and fitted with a fast entry lock for easy sample loading. For this study, Al $K\alpha$ (1486.6 eV) irradiation was used, to prevent overlap of the Fe $2p_{1/2}$ and $2p_{3/2}$ peaks with Fe Auger peaks.

Particle sizes were between 45 and 60 nm, from TEM measurements (JEOL JEM-2100), and the surface area was 16 $\text{m}^2 \text{g}^{-1}$.

3. Results and discussion

We have made a series of methanol oxidation catalysts by doping 1 monolayer (ML for short) of a transition metal oxide onto a haematite support. We have shown previously that iron oxide itself is a combustor for methanol [5,8]. In TPD it shows only H_2O , CO_2 and H_2 as products, the latter two appearing coincidentally, indicating the presence of a surface intermediate formate species which was confirmed by DRIFTS [9,10]. Similarly in reactivity it is only moderately active (T_{50} at 230 °C, where T_{50} is defined as the temperature required for 50% conversion). We have previously shown that dosing Mo onto the surface induces high selectivity to formaldehyde and minimises combustion [8,9]. Here we compare results, under the same conditions for three different TM oxides in order to elucidate what it is that drives selectivity in this reaction.

3.1. Molybdenum

As can be seen in Figure 1, a layer with 1 ML of Mo is very selective to formaldehyde. Conversion begins at very low temperature (~ 140 °C), has a T_{50} of ~ 170 °C and reaches close to full conversion by ~ 250 °C. Selectivity to formaldehyde is high; at low temperatures the other product is dimethyl ether (DME), selectivity to formaldehyde reaches a maximum at ~ 220 °C, and declines after that due mainly to CO production, but CO_2 is also made at higher temperatures. By 390 °C nearly equal amounts of each are produced and the formaldehyde selectivity has dropped to $\sim 15\%$.

Figure 2 shows TPD data after dosing methanol at 40 °C. Here it can be seen that formaldehyde is produced with a peak at ~ 160 °C, but significant amounts of CO are also produced, peaking at 205 °C. This is in contrast to findings for a bulk iron molybdate catalyst where no CO is produced [6].

In many ways the above techniques are the most useful ones for characterising these catalysts because they are the ultimate in surface sensitivity: they only probe the nature of the top monolayer. The 2D nature of the Mo layer makes it impossible to determine structure by XRD. However, there is some infor-

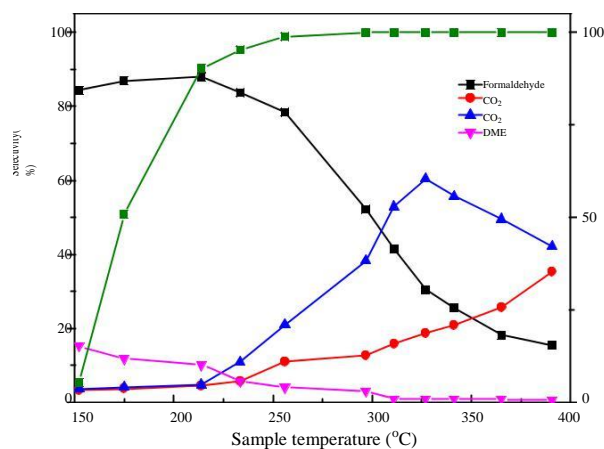


Fig. 1. Selectivity/conversion data for 1 ML $\text{MoO}_x/\text{Fe}_2\text{O}_3$: 50% conversion at 180 °C.

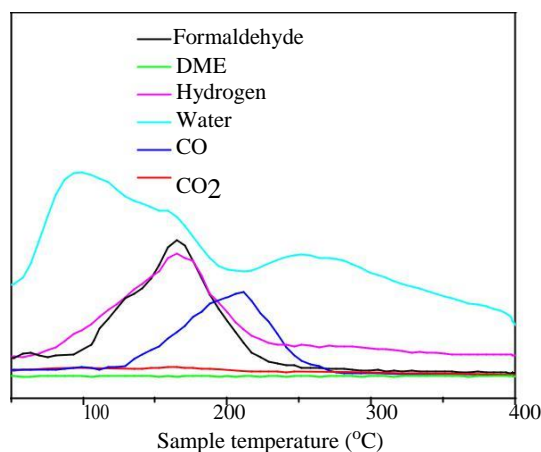


Fig. 2. TPD data for 1 ML MoO_x/Fe₂O₃.

mation from Raman which is sensitive enough to see changes. The limited dimensionality of a 1 ML MoO_x catalyst does not afford any observable peaks by Raman. A 3 ML MoO_x catalyst, however, displays Raman peaks resembling iron molybdate which are partially visible (Figure 3). There are additional bands in the region 780–1000 cm⁻¹ from the Mo layer compared with Fe₂O₃ alone, but due to the low dimensionality they are very broad. However, they seem to be related to bands seen for Fe₂(MoO₄)₃ (780 and 960 cm⁻¹), and there may possibly be bands for MoO₃ (820 and 980 cm⁻¹) too [8,11]. Note that for 3 ML equivalent, only 1 ML remains at the surface as a MoO_x layer, while the other two make Fe₂(MoO₄)₃ layers (~ four such layers), so these dominate the spectrum.

Analysis of XPS data (Figure S1) show Mo to be in its highest oxidation state (Mo₆₊) with Mo 3d_{5/2} binding energy (b.e.) of 232.5 eV: XPS does not provide greater insight into the surface speciation [12,13].

3.2. Vanadium

When 1 ML of V is applied to a haematite support, the re-

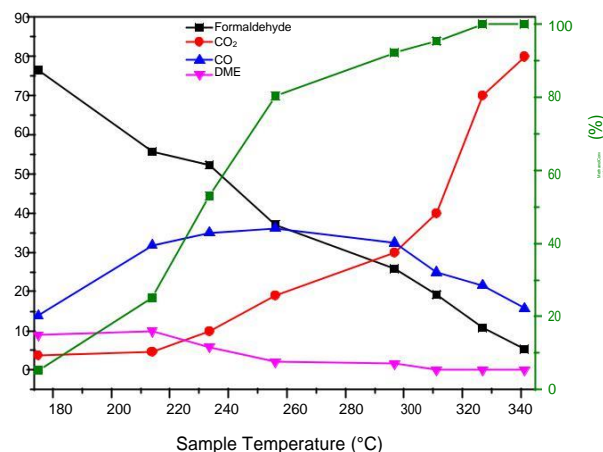


Fig. 4. Selectivity/conversion data for 1 ML VO_x/Fe₂O₃: 50% conversion occurs at 230 °C.

sultant VO_x/Fe₂O₃ catalyst is selective to formaldehyde, albeit not to the degree observed for Mo (Figure 4). Conversion begins in earnest at approximately 180 °C with *T*₅₀ at 230 °C; however, clear differences in product selectivities from Mo are observed. At temperatures up to *T*₅₀, formaldehyde is the major product, with small amounts of DME and CO observed. Above *T*₅₀, however, formaldehyde selectivity decreases rapidly, initially due to increased CO production but then to greater production of CO₂ (rising to 90% CO₂ by 340 °C).

In TPD, 1 ML VO_x/Fe₂O₃ demonstrates strong selectivity to formaldehyde (Figure 5). Formaldehyde and CO are the significant products observed, and little CO₂ is produced, demonstrating that the haematite core is sufficiently shielded to prevent combustion of the methanol, which requires an ensemble of several Fe sites to be available [9]. The ratio of formaldehyde produced to CO produced is poorer than for the equivalent 1 ML MoO_x/Fe₂O₃ catalyst, indicating lower selectivity to formaldehyde for VO_x catalysts: this is to be expected, since Mo is the metal of choice for methanol oxidation catalysts.

Similarly to 1 ML MoO_x/Fe₂O₃, the low dimensionality of the 1 ML VO_x/Fe₂O₃ catalyst renders invisible the peaks which

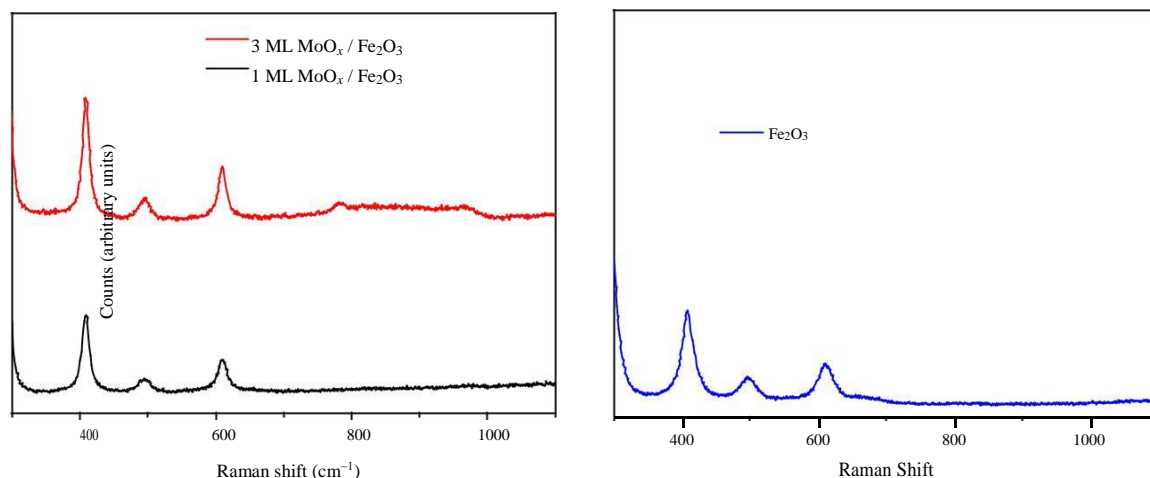


Fig. 3. Left: Raman spectra of 1 and 3 ML MoO_x/Fe₂O₃ – limited dimensionality reduces the Mo contribution to the 1 ML sample spectrum, which shows the core haematite spectrum, but iron molybdate is visible in 3 ML at approximately 780 and 960 cm⁻¹. Right: Raman spectrum of α-Fe₂O₃ for comparison.

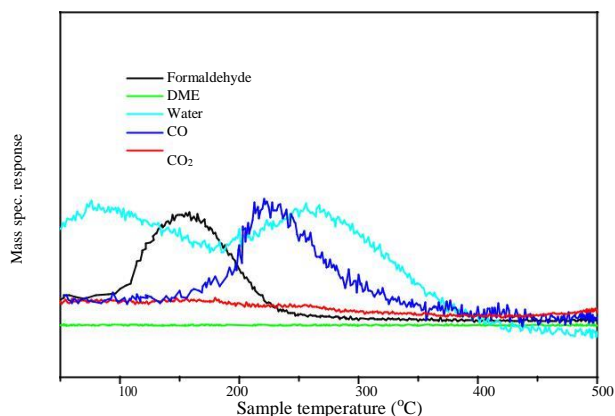


Fig. 5. TPD data for 1 ML VO_x/Fe₂O₃.

could be expected in its Raman spectrum, namely those of V₂O₅ (~700 and 990 cm⁻¹) and FeVO₄ (930–970 cm⁻¹). However, the Raman peaks of FeVO₄ can be seen clearly for the 3ML sample due to the greater quantity of shell material present (Figure 6) [7,14]. XPS analysis of 1 ML VO_x/Fe₂O₃ confirms that each element is present in its highest oxidation state, namely V₅₊ and Fe₃₊ (Figure S2): the 2p_{3/2} peak at ~517 eV confirms this for V [15].

3.3. Niobium

The analogous 1 ML NbO_x/Fe₂O₃ catalyst displays very significant differences from the other two transition metal cations in both pulsed flow reaction and TPD. Pulsed flow reaction of 1 ML NbO_x/Fe₂O₃ gives high selectivity to DME at lower temperatures and conversions, which is superseded by CO₂ production at higher temperatures; however, CO₂ production becomes significant at lower temperatures than equivalent Mo and V catalysts (commencing <200 °C). Some formaldehyde selectivity is seen at low conversions, but it decreases rapidly above 250 °C and is completely absent above 350 °C when conversion is near 100%. The material has much lower reactivity, having a

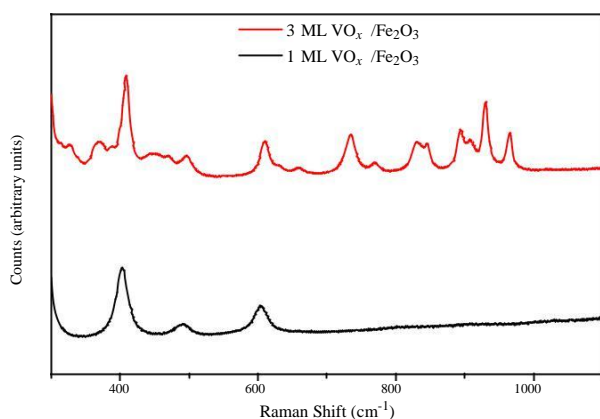


Fig. 6. Raman spectra of 1 and 3 ML VO_x/Fe₂O₃. The limited dimensionality of 1 ML VO_x makes it difficult to see whereas, in contrast, 3 ML displays iron vanadate peaks clearly.

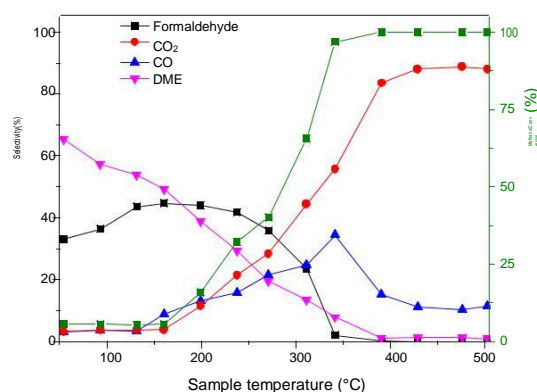


Fig. 7. Selectivity/conversion data for 1 ML NbO_x/Fe₂O₃.

T_{50} of ~300 °C.

In methanol TPD measurements, 1 ML NbO_x/Fe₂O₃ does not produce formaldehyde in any significant quantity (Figure 8). Instead, DME is observed between 200–300 °C, and at higher temperatures mainly H₂, H₂O and CO are seen. Smaller peaks are seen for CO₂, mainly coincident with the CO. In comparison to the CO₂ generated by methanol TPD from Fe₂O₃, they are markedly reduced. This indicates that direct combustion of methanol by the haematite core is partially inhibited, suggesting that the core is not as fully isolated as for Mo and V.

Even for 3 ML NbO_x/Fe₂O₃, the Raman spectrum does not reveal any significant peaks, in contrast to the Mo and V counterparts above (Figure 9). XPS of the samples shows that Nb exists in its highest oxidation state, Nb₅₊, b.e. 207.3 eV (Figure S3), but cannot assist in understanding the apparent differences in catalytic behaviour [16].

3.4. Discussion

TPD is in some ways the most effective technique for verifying that the shell of a second oxide has been obtained on the core material. Due to the inherent differences in catalytic properties between the shell metal oxide and the haematite core, reliable inferences about the state of the surface can be made. It has been reported previously that shell integrity is a key requirement for a selective catalyst [9]. For an iron molybdate

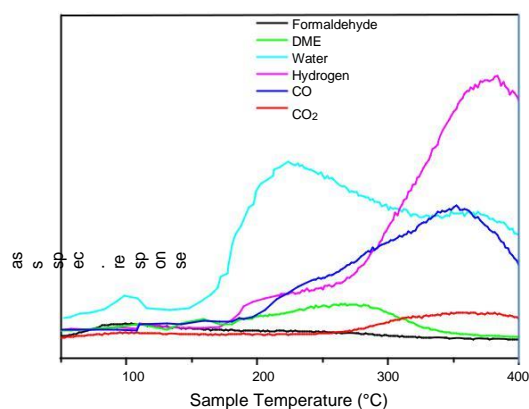


Fig. 8. TPD data for 1 ML NbO_x/Fe₂O₃ under a helium atmosphere.

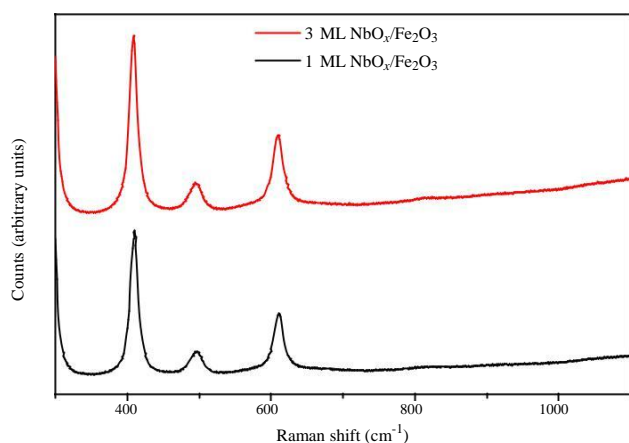


Fig. 9. Raman spectrum of 1 and 3 ML NbO_x/Fe₂O₃.

catalyst with very low Mo content, the surface is not exclusively Mo: instead, there are plentiful neighbouring Fe sites at the surface. In cases where multiple Fe sites can interact directly at the surface, CO₂ is the majority product; the high selectivity of Mo is outcompeted by the higher activity (and worse selectivity) of Fe at the surface [9]. When higher Mo loadings are used, formaldehyde and CO are observed by TPD, but no longer any CO₂. This is a result of the surface becoming increasingly covered with Mo, leaving only occasional isolated Fe sites at the surface amongst the Mo. During reaction, isolated Fe sites produce CO [9]: since neighbouring Fe within range to interact is required for CO₂ production, and due to the high surface oxygen requirement for combustion, no CO₂ is produced [9]. For high Mo loadings, iron molybdate demonstrates selectivity to formaldehyde only, with no other products in TPD under inert gas. An analogous process exists for MoO_x/Fe₂O₃ catalysts and VO_x/Fe₂O₃ catalysts, but for these catalysts small quantities of CO are always observed, indicating that single Fe sites continue to reach the surface [7–9]. We have also shown that Mo remains at the surface in such catalysts by line scans using EELS in an aberration corrected STEM [17], and by EDAX [8].

MoO_x and VO_x/Fe₂O₃ catalysts are both selective to formaldehyde and demonstrate this in their respective TPD results; however, Mo is noticeably superior in this regard to V. This is not unexpected, since Mo is known as the catalyst of choice for formaldehyde production. For 1 ML MoO_x/Fe₂O₃, formaldehyde production is greater than that of CO; however, for 1 ML VO_x/Fe₂O₃, formaldehyde and CO are produced in approximately equivalent quantities. 1 ML NbO_x/Fe₂O₃, however, does not display the same behaviour. It is known that Nb₂O₅ when used as a catalyst generates Brønsted acidic sites, which affect selectivity in the reaction with methanol [18,19]. Catalysts incorporating Nb₂O₅ or similar Nb oxides have been investigated for their ability to produce DME by dehydration, typically using alumina supports [19,20]. While the systems investigated here are designed to be shell-core catalysts on haematite, and not alumina, it is likely that NbO_x would be similarly selective to DME (given that Nb₂O₅ is present, Figure S4). Indeed this is observed in TPD of 1 ML NbO_x/Fe₂O₃, with DME produced at moderate temperatures; however, CO₂ is a significant product

in 1 ML NbO_x TPD. Since CO₂ can only be formed from multiple exposed Fe core sites at the surface, it is clear that 1 ML NbO_x/Fe₂O₃ does not achieve the same degree of core segregation. Nb is visible by XPS, suggesting that Nb is indeed present in the surface layers but does not seem to exist as a layer of NbO_x alone.

Raman spectroscopy is a useful means of determining shell metal oxide speciation, and has greatly benefited studies of other MoO_x and VO_x systems [7,9]. Observation of 1 ML catalysts by Raman can be difficult due to the limited dimensionality of the surface layer at low loadings: instead, Raman spectroscopy is performed on multi-ML systems, whose shells are deep enough for the shell constituents to appear in Raman. We have previously suggested a schematic model for the processes occurring during the calcination of shell-core metal oxide catalysts; we suggest that selective catalysts are generated when their formation proceeds via this model [7,9]. This model suggests that certain intermediate surface phases are formed during calcination at particular temperatures: amorphous oxide units on the haematite surface convert into metal oxide crystallites which then spread evenly to form the MoO_x/VO_x surfaces. At 400 °C for MoO_x and VO_x catalysts, clear signals for MoO₃ and V₂O₅ respectively are seen by Raman at 3 ML coverage (the metal oxide crystallites); however, for NbO_x no such band is observed at any ML coverage (Figure 10). We suggest that the presence of the metal oxide band close to 1000 cm⁻¹, indicative of the terminal M=O species in Raman spectra is a key marker of selectivity to formaldehyde: where it is not seen, neither is selectivity.

Considering the poorer performance of NbO_x/Fe₂O₃ in TPD and pulsed flow reaction, we suggest that Nb cannot be fashioned into a shell-core catalyst in a manner similar to MoO_x/Fe₂O₃ or VO_x/Fe₂O₃ catalysts. The TPD results for NbO_x/Fe₂O₃ are crucial, due to the inherent surface sensitivity of TPD as a technique. CO₂ is not observed for MoO_x and VO_x catalysts, but it is in small quantities for NbO_x. This indicates that the catalyst surface is not as well-formed for Nb in comparison to Mo and V. It is possible that the Nb cannot be as efficiently segregated to the surface layers, leaving portions of the haematite core exposed, or that an alternative iron niobate structure (e.g. Fe_xNb_yO_z) is formed in at the surface with inferior catalytic properties. XRD analysis, however, does not show any differences from haematite, with no iron niobate structures visible. Raman corroborates structural differences during formation through the absence of a visible Nb=O peak at any point during calcination: this suggests that the haematite and Nb form a mixed structure, rather than segregating into separate oxide components as seen for Mo and V. The Tamman temperature, the temperature at which the mobility of species in a solid become significant, could provide the explanation for this behaviour. We have suggested that the formation process for MoO_x and VO_x/Fe₂O₃ catalysts during calcination proceeds stepwise, during which Mo and V diffuse on the surface and aggregate before spreading across the surface to form the desired catalyst structure. The Tamman temperatures for MoO₃ and V₂O₅ (the closest analogues to the systems described here) are 261 and 209 °C respectively [21]: therefore, the calcination

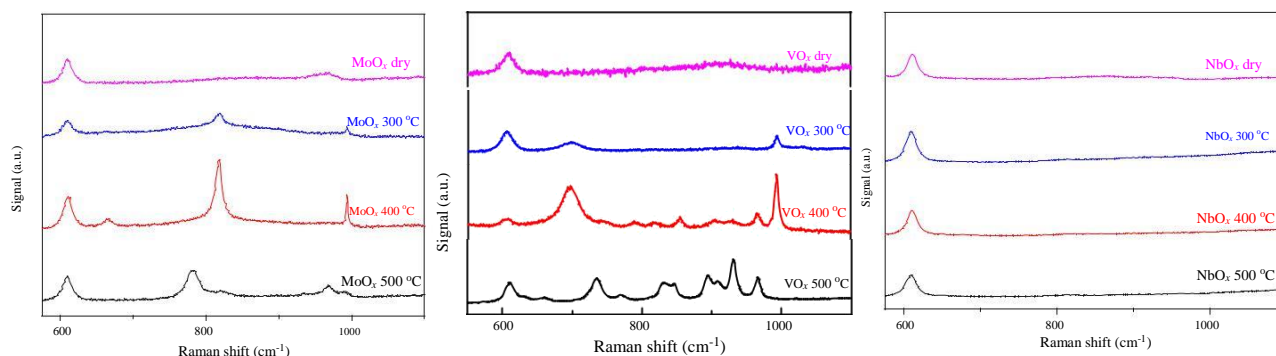


Fig. 10. Comparison of Raman spectra at different points during calcination for 3 ML $\text{NbO}_x/\text{Fe}_2\text{O}_3$, 3 ML $\text{MoO}_x/\text{Fe}_2\text{O}_3$ and 3 ML $\text{VO}_x/\text{Fe}_2\text{O}_3$. In comparison to Mo and V, Nb does not display peaks of interest in Raman: crucially, the Nb=O peak at approx. 1000 cm^{-1} is absent in the $400\text{ }^\circ\text{C}$ $\text{NbO}_x/\text{Fe}_2\text{O}_3$ sample, where it is expected to appear. Both MoO_x and VO_x display this crucial M=O signal at $400\text{ }^\circ\text{C}$ ($\text{M} = \text{Mo/V}$).

temperatures in use will exceed these values, and permit effective diffusion of the Mo and V around the surface. For Nb_2O_5 , however, the Tamman temperature is $620\text{ }^\circ\text{C}$, beyond the maximum $500\text{ }^\circ\text{C}$ used for catalyst calcination [22]. Consequently, the Nb-haematite mixture does not exceed the temperature at which NbO_x will become fully mobile, which may prevent it from forming Nb_2O_5 aggregates necessary at the surface to then spread to form the intended catalyst. In essence, calcination of MoO_x and VO_x finishes the development of the catalyst, resulting in properly formed shell-core catalysts; however, we suggest that NbO_x is unable to complete its formation process at $500\text{ }^\circ\text{C}$, instead remaining improperly formed.

4. Conclusions

Catalysts based on Mo remain the superior catalysts for methanol oxidation to formaldehyde. We have found that V-based catalysts also function as formaldehyde-producing catalysts, but not to the same efficiency as Mo. The shell-core architecture explored initially for Mo catalysts was a means to replicate the surface of the bulk iron molybdate catalyst, but with a greater quantity of surface and less bulk material. Greater surface areas are achieved, alongside significant advantages during analysis (since the analyte of interest, Mo, is present only in the surface layers, non-surface-sensitive, but element-specific techniques become quasi-surface sensitive).

We have subsequently seen that this model system can be extended to V systems, with similar trends in formation, reactivity and characterisation observed. It was expected that Nb, being close to V and Mo in the periodic table, might respond similarly to attempts to fashion it into a shell-core catalyst. In terms of reactivity, Nb_2O_5 is catalytically active, although not selective to formaldehyde (instead displaying acidic behaviour by producing significant amounts of DME). With the current synthetic methodology, Nb seems unable to form a fully selective $\text{NbO}_x/\text{Fe}_2\text{O}_3$ catalyst; instead, the $\text{NbO}_x/\text{Fe}_2\text{O}_3$ catalyst produces CO_2 by TPD alongside selective product DME. We suggest this is due to its vastly greater Tamman temperature, and the consequent inability of NbO_x to diffuse as easily as Mo

and V across the surface of the haematite during calcination.

Acknowledgments

The authors thank HarwellXPS, the EPSRC National Facility for X-Ray Photoelectron Spectroscopy, for their assistance in performing XPS measurements, and EPSRC for support via the UK Catalysis Hub (EP/K014854/1, EP/K014714/1), and EPSRC and Diamond Light Source for funding the studentship to PH.

References

- [1] G. A. Olah, A. Goeppert, G. K. S. Prakash, *Beyond Oil and Gas: The Methanol Economy*, John Wiley & Sons, Ltd, **2009**, 179–184.
- [2] MefCO2.eu (accessed 26 January 2019).
- [3] K. V. Raun, L. F. Lundegaard, J. Chevallier, P. Beato, C. C. Appel, K. Nielsen, M. Thorhauge, A. D. Jensen, M. Høj, *Catal. Sci. Technol.*, **2018**, 8, 4626–4637.
- [4] M. F. Portela, A. Kiennemann, *Catal. Rev.-Sci. Eng.*, **2005**, 47, 125–174.
- [5] M. Bowker, R. Holroyd, A. Elliott, P. Morrall, A. Alouche, C. Entwistle, A. Toerncrona, *Catal. Lett.*, **2002**, 83, 165–176.
- [6] M. P. House, A. F. Carley, R. Echevarria-Valda, M. Bowker, *J. Phys. Chem. C*, **2008**, 112, 4333–4341.
- [7] P. Hellier, P. P. Wells, D. Gianolio, M. Bowker, *Top. Catal.*, **2018**, 61, 357–364.
- [8] C. Brookes, P. P. Wells, G. Cibi, N. Dimitratos, W. Jones, D. J. Morgan, M. Bowker, *ACS Catal.*, **2014**, 4, 243–250.
- [9] M. Bowker, M. House, A. Alshehri, C. Brookes, E. K. Gibson, P. P. Wells, *Catal. Struct. React.*, **2015**, 1, 95–100.
- [10] M. Bowker, E. K. Gibson, I. P. Silverwood, C. Brookes, *Faraday Discuss.*, **2016**, 188, 387–398.
- [11] L. Seguin, M. Figlarz, R. Cavagnat, J.-C. Lassègues, *Spectrochim. Acta Part A*, **1995**, 51, 1323–1344.
- [12] J. G. Choi, L. T. Thompson, *Appl. Surf. Sci.*, **1996**, 93, 143–149.
- [13] W. Gruenert, A. Y. Stakheev, R. Feldhaus, K. Ers, E. S. Shpiro, K. M. Minachev, *J. Phys. Chem.*, **1991**, 95, 1323–1328.
- [14] K. Routray, W. Zhou, C. J. Kiely, I. E. Wachs, *ACS Catal.*, **2011**, 1, 54–66.
- [15] G. Silversmit, D. Depla, H. Poelman, G. B. Marin, R. De Gryse, *J. Electron Spectrosc. Relat. Phenom.*, **2004**, 135, 167–175.
- [16] V. V. Atuchin, I. E. Kalabin, V. G. Kesler, N. V. Pervukhina, *J. Electron Spectrosc. Relat. Phenom.*, **2005**, 142, 129–134.

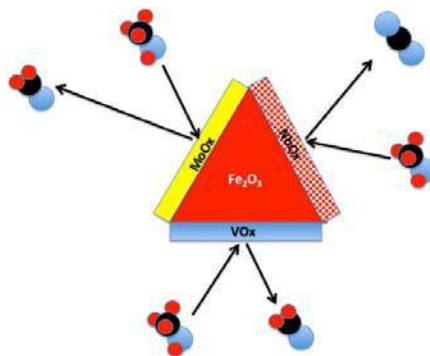
Graphical Abstract

Methanol oxidation over shell-core $\text{MO}_x/\text{Fe}_2\text{O}_3$ ($\text{M} = \text{Mo}, \text{V}, \text{Nb}$) catalysts

Pip Hellier, Peter P. Wells, Michael Bowker *

UK Catalysis Hub, UK; Cardiff University, UK; University of Southampton, UK; Diamond Light Source Ltd, UK

Methanol oxidation on three surface oxides on Fe_2O_3 showing the main carbon products. Mo and V monolayers are selective to formaldehyde, while Nb does not make complete monolayers and mainly combusts to CO_2 .



[17] M. P. House, M. D. Shannon, M. Bowker, *Catal. Lett.*, **2008**, 122, 210–213.

[18] D. Liu, C. Yao, J. Zhang, D. Fang, D. Chen, *Fuel*, **2011**, 90, 1738–1742.

[19] T. Kitano, T. Shishido, K. Teramura, T. Tanaka, *J. Phys. Chem. C*, **2012**, 116, 11615–11625.

[20] Q. Sun, Y. Fu, H. Yang, A. Auroux, J. Shen, *J. Mol. Catal. A*, **2007**, 275, 183–193.

[21] K. Chen, A. T. Bell, E. Iglesia, *J. Phys. Chem. B*, **2000**, 104, 1292–1299.

[22] I. E. Wachs, Y. Chen, J. M. Jehng, L. E. Briand, T. Tanaka, *Catal. Today*, **2003**, 78, 13–24.

核壳结构 $\text{MO}_x/\text{Fe}_2\text{O}_3$ ($\text{M} = \text{Mo}, \text{V}, \text{Nb}$)催化剂上甲醇氧化反应

Pip Hellier ^{a,b}, Peter P. Wells ^{c,d}, Michael Bowker ^{a,b,*}

^a卢瑟福-阿普尔顿实验室, 哈韦尔研究综合体, 英国催化中心, 哈韦尔, 英国

^b卡迪夫大学化学学院, 卡迪夫, 英国

^c南安普顿大学化学学院, 南安普顿, 英国

^d哈韦尔科学与创新园区, 钻石光源有限公司, 迪德科特, 英国

摘要: 本文比较了赤铁矿为核, Mo, V和Nb氧化物为壳层的材料在选择性甲醇氧化反应中的性能。

Mo和V对甲醛都有很高的选择性, 而Nb则没有。Nb的反应模式非常不同, 主要表现为脱氢(生成CO)和脱水(生成三甲醚), 表明缺乏完整的壳层, 同时Raman光谱发现, NbO_x 的形成过程与Mo和V的并不相同。

我们推测这是由于固体材料在形成过程中的流动性差异很大, NbO_x 需要明显较高(和有害)的焙烧温度, 以便为壳层的形成提供足够的流动性。**关键词:** 甲醇; 氧化; 甲醛; 钼酸铁; 核壳结构催化剂

收稿日期: 2019-01-31. 接受日期: 2019-03-05. 出版日期: 2019-00-05.

*通讯联系人. 电子信箱: bowkerm@cardiff.ac.uk

本文的电子版全文由Elsevier出版社在ScienceDirect上出版(<http://www.sciencedirect.com/science/journal/18722067>).

For Author Index:

HELLIER Pip, WELLS Peter P., BOWKER Michael

Methanol oxidation over shell-core $\text{MO}_x/\text{Fe}_2\text{O}_3$ ($\text{M} = \text{Mo}, \text{V}, \text{Nb}$) catalysts

Pip Hellier ^{a,b}, Peter P. Wells ^{c,d}, Michael Bowker ^{a,b,*}

^a UK Catalysis Hub, Research Complex at Harwell, Rutherford Appleton Laboratory, Harwell,

UK ^b School of Chemistry, Cardiff University, Cardiff, UK

^c School of Chemistry, University of Southampton, Southampton, UK

^d Diamond Light Source Ltd, Harwell Science and Innovation Campus, Didcot, UK

* Corresponding author. E-mail: bowkerm@cardiff.ac.uk

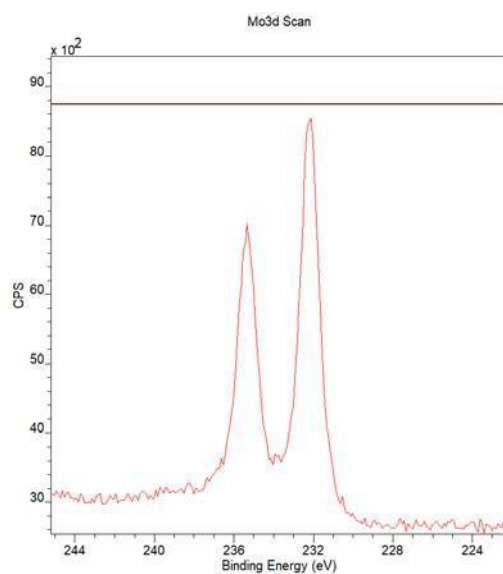


Fig. S1. Mo region of XPS data from 1 ML $\text{MoO}_x/\text{Fe}_2\text{O}_3$.

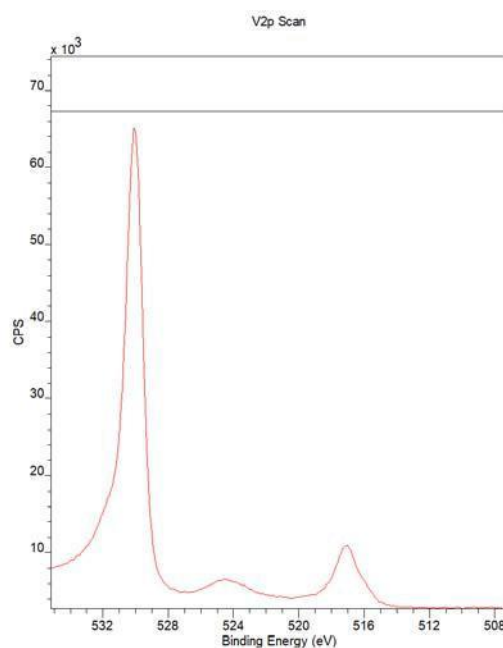


Fig. S2. V region of XPS data from 1 ML $\text{VO}_x/\text{Fe}_2\text{O}_3$.

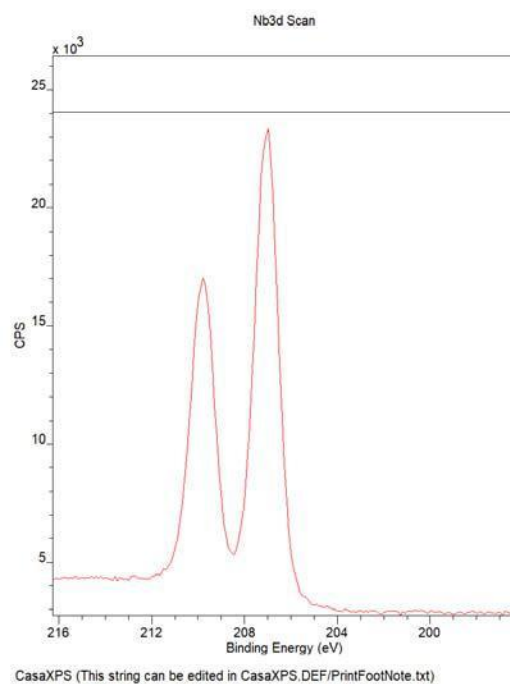


Fig. S3. Nb region of XPS data from 1 ML NbO_x/Fe₂O₃.

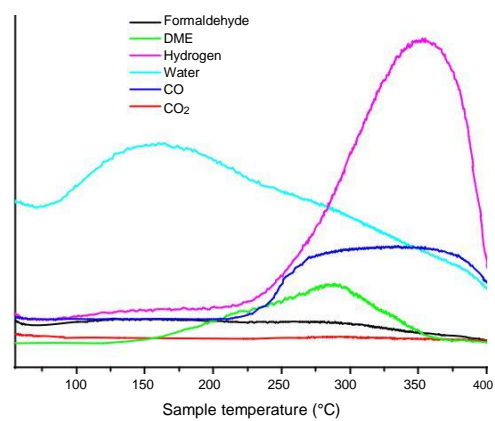


Fig. S4. TPD data for Nb₂O₅ calcined to 500°C. Major products are DME and CO – no significant CO₂ is produced.